

[³H]DAMGO (Amersham)¹⁸. Measurements were done in triplicate. Binding data was analysed using the LIGAND program (supplied by P. Munson).

In situ hybridization

Cryostat sections (13 μm) of fresh brain tissue were hybridized with ³⁵S-labelled oligonucleotide probes specific for the dopamine D1 and D2 receptors¹ (see Supplementary Information).

Immunohistochemistry

Mice were anaesthetized with sodium pentobarbital and fixed transcardially with 4% paraformaldehyde in 0.1 M phosphate buffer, the brains removed and sections cut at 40 μm for processing with antibodies against the mu opiate receptor (Chemicon), c-Fos or Fos-B (Santa Cruz). The Fos-B antibody recognizes both full-length and truncated products of the gene. To study Fos-B expression, mice were treated daily with two injections of morphine in increasing doses (20, 40, 60, 80 mg kg⁻¹). On the last day, a single dose of 100 mg kg⁻¹ was given in the morning and mice were perfused 6 h later.

Received 30 September 1999; accepted 2 March 2000.

1. De Felipe, C. *et al.* Altered nociception, analgesia and aggression in mice lacking the receptor for substance P. *Nature* **392**, 394–397 (1998).
2. Kramer, M. S. *et al.* Distinct mechanism for antidepressant activity by blockade of central substance P receptors. *Science* **281**, 1640–1645 (1998).
3. Culman, J., Klee, S., Ohlendorf, C. & Unger, T. Effect of tachykinin receptor inhibition in the brain on cardiovascular and behavioural responses to stress. *J. Pharmacol. Exp. Ther.* **280**, 238–246 (1997).
4. Nakaya, Y. *et al.* Immunohistochemical localization of substance P receptor in the central nervous system of the adult rat. *J. Comp. Neurol.* **347**, 249–274 (1994).
5. Wise, R. A. Neurobiology of addiction. *Curr. Opin. Neurobiol.* **6**, 243–251 (1996).
6. Robbins, T. W. & Everitt, B. J. Drug addiction: bad habits add up. *Nature* **398**, 567–570 (1999).
7. Koob, G. F., Sanna, P. P. & Bloom, F. E. Neuroscience of addiction. *Neuron* **21**, 467–476 (1998).
8. Koob, G. K. & Le Moal, M. Drug abuse: Hedonic homeostatic dysregulation. *Science* **278**, 52–70 (1997).
9. Gerfen, C. R. Substance P (neurokinin-I) receptor mRNA is selectively expressed in cholinergic neurons in the striatum and basal forebrain. *Brain Res.* **556**, 165–170 (1991).
10. Maldonado, R. *et al.* Absence of opiate rewarding effects in mice lacking dopamine D2 receptors. *Nature* **388**, 586–589 (1995).
11. Baik, J. H. *et al.* Parkinsonian-like locomotor impairment in mice lacking dopamine D2 receptors. *Nature* **377**, 424–428 (1995).
12. Wise, R. A. & Bozarth, M. A. A psychomotor stimulant theory of addiction. *Psychol. Rev.* **97**, 469–492 (1987).
13. Bechara, A. & van der Kooy, D. A single brain stem substrate mediates the motivational effects of both opiates and food in nondeprived rats but not in deprived rats. *Behav. Neurosci.* **106**, 351–363 (1992).
14. Maldonado, R., Girdlestone, D. & Roques, B. P. RP 67580, a selective antagonist of neurokinin-1 receptors, modifies some of the naloxone-precipitated morphine withdrawal signs in rats. *Neurosci. Lett.* **156**, 135–140 (1993).
15. Matthes, H. W. D. *et al.* Loss of morphine-induced analgesia, reward effect and withdrawal symptoms in mice lacking the m-opioid-receptor gene. *Nature* **383**, 819–823 (1996).
16. Rupniak, N. M. J. *et al.* A Pharmacological blockade or genetic deletion of substance P (NK1) receptors attenuates neonatal vocalisation in guinea-pigs and mice. *Neuropharmacology* (in the press).
17. Maldonado, R., Stimus, L., Gold, L. & Koob, G. F. Role of different brain structures in the expression of the physical morphine withdrawal syndrome. *J. Pharmacol. Exp. Ther.* **261**, 669–677 (1992).
18. Bozarth, M. A. Physical dependence produced by central morphine infusions: an anatomical mapping study. *Neurosci. Biobehav. Rev.* **18**, 373–383 (1994).
19. Mansour, A., Fox, C. A., Burke, S., Akil, H. & Watson, S. J. Immunohistochemical localization of the cloned mu opioid receptor in the rat CNS. *J. Chem. Neuroanat.* **8**, 283–305 (1995).
20. Kieffer, B. L., Beford, K., Gaveriaux-Ruff, C. & Hirth, C. G. The delta-opioid receptor: isolation of a cDNA by expression cloning and pharmacological characterization. *Proc. Natl Acad. Sci. USA* **89**, 12048–12052 (1992).
21. Izenwasser, S., Buzas, B. & Cox, B. M. Differential regulation of adenylyl cyclase activity by mu and delta opioids in rat caudate putamen and nucleus accumbens. *J. Pharmacol. Exp. Ther.* **267**, 145–152 (1993).
22. Nye, H. E. & Nestler, E. J. Induction of chronic Fos-related antigens in rat brain by chronic morphine administration. *Mol. Pharmacol.* **49**, 636–645 (1996).
23. Kelz, M. B. *et al.* Expression of the transcription factor delta FosB in the brain controls sensitivity to cocaine. *Nature* **401**, 272–276 (1999).
24. Aubry, J. M., Schulz, M. F., Pagliusi, S., Schulz, P. & Kiss, J. Z. Coexpression of dopamine D2 and substance P (neurokinin-1) receptor messenger RNAs by a subpopulation of cholinergic neurons in the rat striatum. *Neuroscience* **53**, 417–424 (1993).
25. Graybiel, A. M., Aosaki, T., Flaherty, A. W. & Kimura, M. The basal ganglia and adaptive motor control. *Science* **265**, 1826–1831 (1994).
26. Elliott, P. J. & Iversen, S. D. Behavioural effects of tachykinins and related peptides. *Brain Res.* **381**, 68–76 (1986).
27. Boix, F., Sandor, P., Nogueira, P. J., Huston, J. P. & Schwarting, R. K. Relationship between dopamine release in nucleus accumbens and place preference induced by substance P injected into the nucleus basalis magnocellularis region. *Neuroscience* **64**, 1054–1055 (1995).
28. Shaham, Y. & Stewart, J. Stress reinstates heroin-seeking in drug-free animals: an effect mimicking heroin, not withdrawal. *Psychopharmacol.* **119**, 334–341 (1995).

Supplementary information is available on Nature's World Wide Web site (<http://www.nature.com>) or as a paper copy from the London editorial office of Nature.

Acknowledgements

We thank J. O'Brien, J. A. Perez De Gracia, and P. Mantyh, R. Maldonado and C. Stanford

for reading and commenting on the manuscript, and N. Rupriak for sharing unpublished data.

Correspondence and requests for materials should be sent to S.P.H. (e-mail: hunt@ucl.ac.uk).

Vanilloid receptor-1 is essential for inflammatory thermal hyperalgesia

John B. Davis*, **Julie Gray***, **Martin J. Gunthorpe***, **Jonathan P. Hatcher***, **Phil T. Davey***, **Philip Overend†**, **Mark H. Harries***, **Judi Latcham‡**, **Colin Clapham§**, **Kirsty Atkinson§**, **Stephen A. Hughes§**, **Kim Rance§**, **Evelyn Grau§**, **Alex J. Harper***, **Perdita L. Pugh***, **Derek C. Rogers***, **Sharon Bingham***, **Andrew Randall*** & **Steven A. Sheardown§**

*Departments of *Neuroscience Research, †Statistical Sciences, ‡Laboratory Animal Sciences and §Biotechnology & Genetics, SmithKline Beecham Pharmaceuticals, Third Avenue, Harlow CM19 5AW, UK*

The vanilloid receptor-1 (VR1) is a ligand-gated, non-selective cation channel expressed predominantly by sensory neurons. VR1 responds to noxious stimuli including capsaicin, the pungent component of chilli peppers, heat and extracellular acidification, and it is able to integrate simultaneous exposure to these stimuli^{1,2}. These findings and research linking capsaicin with nociceptive behaviours (that is, responses to painful stimuli in animals³ have led to VR1 being considered as important for pain sensation. Here we have disrupted the mouse VR1 gene using standard gene targeting techniques. Small diameter dorsal root ganglion neurons isolated from VR1-null mice lacked many of the capsaicin-, acid- and heat-gated responses that have been previously well characterized in small diameter dorsal root ganglion neurons from various species. Furthermore, although the VR1-null mice appeared normal in a wide range of behavioural tests, including responses to acute noxious thermal stimuli, their ability to develop carrageenan-induced thermal hyperalgesia was completely absent. We conclude that VR1 is required for inflammatory sensitization to noxious thermal stimuli but also that alternative mechanisms are sufficient for normal sensation of noxious heat.

We have used homologous recombination in embryonic stem (ES) cells to generate a mouse lacking transmembrane domains 2–4 of the mVR1 gene (Fig. 1a). Germline chimaeras were crossed onto C57Bl/6J females to generate heterozygotes, which were intercrossed giving rise to overtly healthy homozygous mutant offspring in the expected mendelian ratio (average litter numbers: VR1^{-/-}, 2.5 ± 0.36; VR1^{+/-}, 4.9 ± 0.40; VR1^{+/+}, 2.5 ± 0.23; n = 28). Successful targeting of the locus and germline transmission was confirmed by Southern analysis (Fig. 1b) and by polymerase chain reaction (PCR) (Fig. 1c).

The expression of VR1 in sensory neurons from dorsal root ganglia has been previously established using both messenger RNA analysis and immunocytochemistry^{1,2}. In addition, numerous pharmacological assays using vanilloid receptor agonists, such as capsaicin and resiniferatoxin, and antagonists, such as capsazepine⁴, have demonstrated the presence of functional VR1 in small diameter dorsal root ganglion (sDRG) neurons⁵. We have used a similar functional approach to confirm the elimination of VR1-mediated responses in our VR1-null mice. Dissociated neuronal cultures were prepared from the DRG of VR1 wild type (VR1^{+/+}), VR1 heterozygote (VR1^{+/-}) or VR1-null (VR1^{-/-}) littermates. After 20–40 h in culture, electrophysiological recordings of responses to a range of stimuli were made from the classically nociceptive, small DRG neurons (diameter <22 μm, mean capacitance 9.4 ± 0.5 pF).

Responses to capsaicin (1 μM) were present in 74% ($n = 34$) of sDRG neurons from $\text{VR1}^{+/+}$ mice. A similar number (62%, $n = 21$; data not shown) from $\text{VR1}^{+/-}$ mice also responded to capsaicin, with currents indistinguishable in size or waveform from those observed in $\text{VR1}^{+/+}$ cells. In contrast, capsaicin failed to elicit a response in any of the 29 cells tested from $\text{VR1}^{-/-}$ cultures (Fig. 2).

In 9 out of 13 cells from $\text{VR1}^{+/+}$ cultures a transient extracellular acidification to pH 5.3 produced a slowly developing, non-desensitizing, inward current. This current had kinetics that closely resembled the slow acid-gated current observed in primary rat DRG neurons⁶, or in HEK 293 cells or *Xenopus* oocytes expressing VR1 (ref. 1). This slow acid-gated current was not observed in any cells that did not respond to capsaicin. In 46% of cells from $\text{VR1}^{+/+}$ cultures, however, an additional rapidly activating and desensitizing inward current was also observed at the onset of a response to pH 5.3. This transient current component was found in both capsaicin-responsive and -unresponsive cells and probably represents the activation of channels belonging to the acid-sensing ionic channel (ASIC) family⁷. In all $\text{VR1}^{-/-}$ cells examined, the slowly activating pH 5.3-gated response was absent. In contrast, the rapidly activating ASIC-type current was still seen in a proportion of cells (see Fig. 2a). These data support the hypothesis that a principal part of the maintained (that is, non-desensitizing) acid-gated excitations of sDRG neurons reflects the activity of VR1. This finding also indicates that VR1 may be important in generating acidosis-related pain.

Although lacking the expected responses to pH 5.3 and capsaicin, $\text{VR1}^{-/-}$ cells responded normally to two neurotransmitters, GABA (γ -aminobutyric acid, 100 μM) and ATP (50 μM), that have been previously shown to activate ion channels in sensory neurons^{8,9}. The

responses to these agents were present in a similar percentage of $\text{VR1}^{+/+}$ and $\text{VR1}^{-/-}$ cells (Fig. 2b). Furthermore, no marked differences in response amplitudes or kinetics were noted when recordings from $\text{VR1}^{+/+}$ and $\text{VR1}^{-/-}$ cells were compared. Notably, the responses to ATP in both $\text{VR1}^{+/+}$ and $\text{VR1}^{-/-}$ sDRG neurons exhibited the rapid desensitization kinetics typical of capsaicin-responsive sDRG neurons⁹.

Heterologously expressed recombinant VR1, in addition to responding to capsaicin, acidic pH and anandamide, is activated by increases in temperature to levels above $\sim 44^\circ\text{C}$ (refs 1, 10). Similar heat-activated currents have been reported in capsaicin-responsive sDRG neurons^{11,12}. To test the contribution of VR1 to these thermal responses, we compared the heat-gated currents generated by 2-s step increases in temperature, from room temperature (23.5–25.5 $^\circ\text{C}$) up to 54 $^\circ\text{C}$, in $\text{VR1}^{+/+}$ and $\text{VR1}^{-/-}$ sDRG neurons. As reported¹¹, the heat-activated current exhibits two components (Fig. 3a, top two panels). The first component shares characteristics with currents mediated by recombinant VR1, including a well defined activation threshold at $\sim 44^\circ\text{C}$ and substantial outward rectification. The second has been ascribed to a 'non-specific' change in membrane or seal resistance¹¹. This latter current does not exhibit a marked activation threshold¹¹, is associated with little or no change in current variance and has an amplitude directly proportional to the pre-stimulus holding current (and input resistance). Such non-specific heat-gated currents can also be observed in capsaicin-unresponsive sDRG neurons as well as in other cell types.

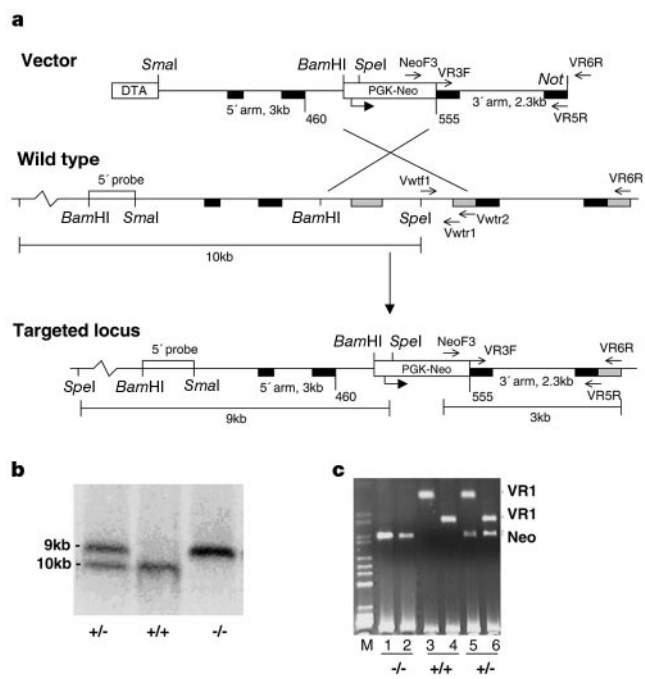


Figure 1 Disruption of VR1 gene by homologous recombination. **a**, Diagram of targeting construct and strategy. Exons are indicated as black boxes. Shaded boxes represent exon sequences not present in the targeting construct. The diagnostic PCR product and *SpeI* cleavage fragments are indicated with the 3' external PCR primer VR6R and the 5' external *Bam*HI/*Sma*I probe (open box). **b**, Representative example of genomic Southern blot from wild type (+/+), heterozygous mutant (+/-) and homozygous mutant (-/-) mouse tail DNA cleaved with *SpeI* and hybridized with a ³²P-labelled *Bam*HI/*SpeI* 5' external probe. **c**, Wild type (+/+), heterozygous mutant (+/-) and homozygous mutant (-/-) mouse tail DNA genotyped by multiplex PCR. All samples contained neo-specific primers. Lanes 1, 3 and 5 contain wild-type VR1-specific primers Vwtr1 and Vwtr2. Lanes 2, 4 and 6 contain wild-type VR1-specific primers Vwtr1 and Vwtr2.

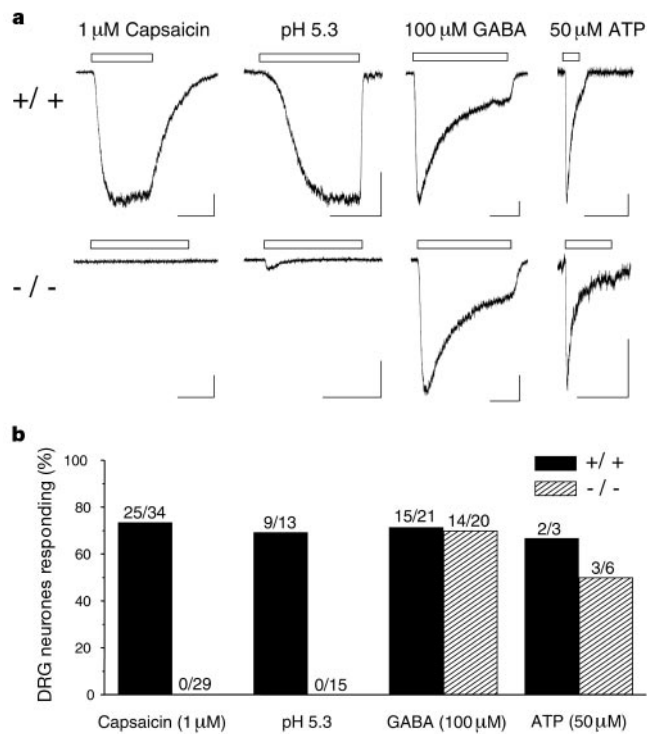


Figure 2 Ligand-gated currents in sDRG neurons from $\text{VR1}^{+/+}$ and $\text{VR1}^{-/-}$ mice. **a**, Whole-cell patch-clamp recordings of inward currents recorded in sDRG neurons, from $\text{VR1}^{+/+}$ or $\text{VR1}^{-/-}$ mice, in response to the application of capsaicin (1 μM), protons (extracellular acidification to pH 5.3), GABA (100 μM) or ATP (50 μM) for the time indicated by the bar. Vertical scale bar represents 200 pA for currents recorded in response to capsaicin, pH 5.3 and GABA, and 50 pA for ATP-gated current. The horizontal scale bar represent 5 s in all cases. **b**, Pooled data from all $\text{VR1}^{+/+}$ (black bars) and $\text{VR1}^{-/-}$ (hatched bars) DRG neurons studied indicating the percentage of cells responsive to the application of either capsaicin, GABA or ATP, or yielding a sustained response to protons.

Increases in temperature (from 25 to 54 °C) in both VR1^{+/+} and VR1^{-/-} sDRG neurons consistently produced a heat-activated inward current. In a proportion of VR1^{+/+} cells, the current elicited had an amplitude that was linearly related to the applied temperature (Fig. 3a, top) and was thus attributable to the non-specific current. In the remaining VR1^{+/+} sDRG neurons, a clear additional current component was recruited at temperatures above a threshold of ~44 °C (Fig. 3a, middle, and 3b). The proportion of VR1^{+/+} cells exhibiting this additional heat-gated current (15 out of 33) was similar to the proportion of capsaicin-responsive cells (5 out of 11) in the same preparation (~50%). Pooled data comparing the heat-gated responses at 49–50 °C in VR1^{+/+} with VR1^{-/-} sDRG neurons show that no VR1^{-/-} cells responded with a response greater than 200% of the holding current at room temperature (mean 79 ± 10%), whereas this level was surpassed in almost 50% of VR1^{+/+} cells (Fig. 3c). The lack of a ‘specific’ current in VR1^{-/-} sDRG neurons strongly supports previous suggestions that a current with its characteristics arises from the thermal activation of VR1 (ref. 12).

On the basis of its heat-dependent gating, VR1 has been proposed to be a sensor for noxious heat¹. To specifically address this hypothesis, we compared the thermoresponsive behaviour of VR1^{+/+}, VR1^{-/-} and VR1^{+/-} mice, both acutely and after the experimental induction of inflammation. The latency of response to an acute thermal stimulus was measured using a 50 or 52.5 °C hotplate (Fig. 4a), or a focused radiant heat stimulus (Fig. 4c,d). All of the mice studied responded to these previously well characterized noxious stimuli.

Increasing the temperature of the hotplate decreased the latency of response for all genotypes (Fig. 4a, $F = 24.91$; d.f. = 1,49; $P < 0.001$). Unexpectedly, neither VR1^{-/-} mice ($P = 0.16$ and $P = 0.06$, 50 and 52.5 °C, respectively) nor VR1^{+/-} mice ($P = 0.52$ and $P = 0.08$, 50 and 52.5 °C, respectively) showed a significant difference when compared with VR1^{+/+} mice in hotplate responses (Fig. 4a). Similarly, there were no significant differences between genotypes in

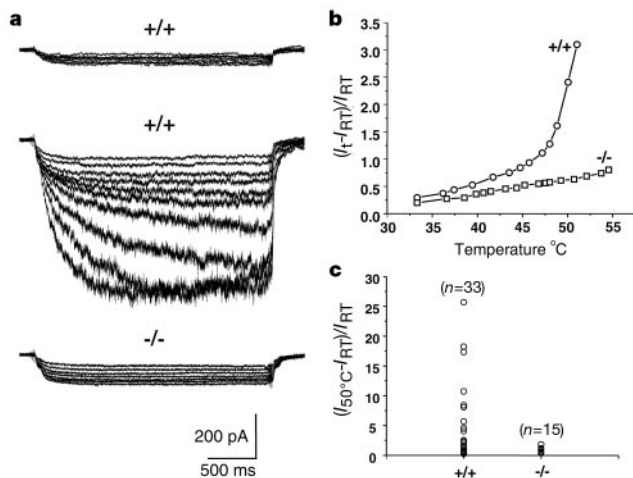


Figure 3 Heat-gated currents in sDRG neurons from VR1^{+/+} and VR1^{-/-} mice. **a**, Example of heat-activated currents from three different sDRGs. Top traces, a VR1^{+/+} cell lacking a detectable threshold-dependent heat-activated current (temperature range 33–54 °C); middle traces, a VR1^{+/+} cell exhibiting a clear threshold-gated current (temperatures 33.3, 37.4, 41.7, 44.8, 45.7, 47.2, 48.8, 50.1, 51 °C); bottom trace, a typical VR1^{-/-} cell (temperature range 33–54 °C). **b**, Plot of applied-heat versus evoked current for the responsive VR1^{+/+} and VR1^{-/-} cells shown in **a**. The peak amplitude for each temperature has been normalized to the pre-stimulus room-temperature (RT) holding current. **c**, Scatter plot showing the increase in current amplitude produced by a temperature jump to 49–50 °C. Data points are normalized to the pre-stimulus room-temperature holding current. Note the significant population of VR1^{+/+} cells exhibiting a heat-gated response greater than 200% of holding current. These cells all possessed a slowly activating high-variance current akin to that shown in the middle panel of **a**.

terms of response to a radiant heat stimulus set at an intensity that produces a paw-withdrawal latency of ~9 s in normal mice (Fig. 4c). However, the analysis of variance of the effect of genotype upon response latency at 52.5 °C ($F = 3.11$; d.f. = 2,49 $P = 0.053$) only just failed to reach significance. Thus, although it is clear that mice lacking VR1 are still able to respond to noxious heat, there remains a possibility that subtle differences in the behavioural responses to different intensities of heat may occur. Such an effect may be masked to some degree by the mixed strain background of the N1F1 cohort that we used in these studies.

Our data give rise to a paradox because although the electrophysiological response specific to noxious temperatures was absent in the VR1^{-/-} sDRG neurons the null mice responded normally to noxious heat. Neonatal treatment with capsaicin, which ablates the capsaicin-sensitive nociceptors, results in significant analgesia towards thermal stimuli¹³, suggesting that the VR1-expressing nociceptors are essential for normal thermal nociception. Future work may help to explain the paradox, for example, by characterization of the DRG cell types responsible for transducing the retained thermal sensation or by the discovery of another heat sensor whose function may be lost or compromised in cell culture. Vanilloid-receptor like 1 (VRL-1), which has also been reported as a heat receptor¹⁴, may contribute to the retained response. VRL-1 has a higher threshold for activation (~52 °C compared with 42 °C for VR1 *in vitro*)¹⁴ and may therefore be unlikely to have a significant

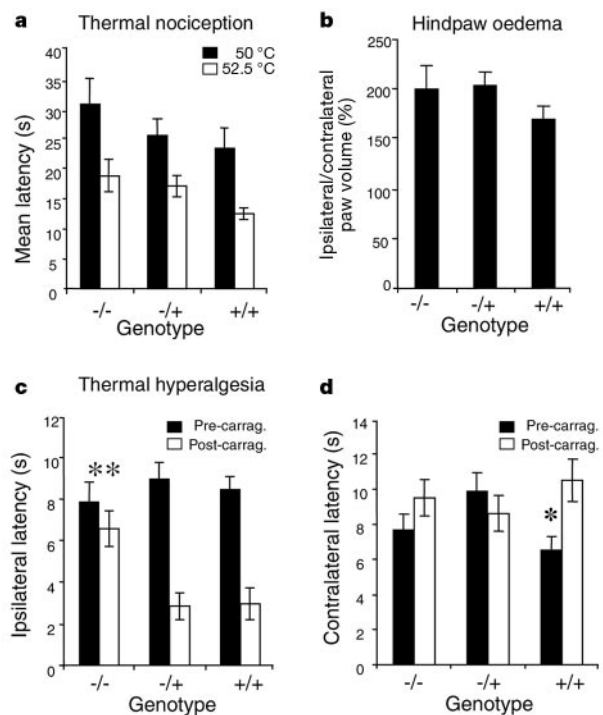


Figure 4 Responses to thermal stimuli in normal and sensitized animals. **a**, Normal nociceptive behaviour to noxious thermal stimuli. Withdrawal or licking latencies in the hotplate assay at 50 or 52.5 °C. No significant differences were seen between wild-type (+/+; $n = 8$ and 9 for 50 °C and 52.5 °C, respectively), heterozygous (-/+; $n = 10$ and 10 , respectively), or homozygous mutant (-/-; $n = 10$ and 9 , respectively) mice.

b, Measurement of paw volume after injection of carrageenan. Ipsilateral volume is expressed as a percentage of the uninjected contralateral paw ($n = 10$ for each group). **c**, Ipsilateral withdrawal latencies before or 4 h after carrageenan injection, in response to focused radiant heat. VR1^{-/-} mice showed a highly significant reversal of hyperalgesia when compared with VR1^{+/+} mice; two asterisks, $P < 0.001$. **d**, Contralateral withdrawal latencies before or after carrageenan injection, in response to radiant heat. VR1^{+/+} ($n = 17$) but not VR1^{-/-} ($n = 18$) or VR1^{+/-} ($n = 20$) mice show a significant hypoalgesic effect; asterisk, $P < 0.05$.

role in the heat responses described above. Developmental adaptation in the VR1-null mice, or uncharacterized properties of VRL-1 *in vivo*, however, can not be ruled out at this stage. Single or double genetic knockout approaches may shed further light on the relative contributions of VR1, VRL-1 or other molecular heat detectors.

A hyperalgesic response to thermal stimuli is associated with inflammation and was tested for using intraplantar carrageenan injection into the hindpaw and subsequent stimulation by radiant heat¹⁵. Analysis of the degree of carrageenan-induced hindpaw inflammation showed no significant differences in swelling between VR1^{-/-} and VR1^{+/+} or VR1^{+/-} animals (Fig. 4b). Four hours after carrageenan injection, VR1^{+/+} mice and VR1^{+/-} mice exhibited a highly significant decrease in paw-withdrawal latencies compared with baseline pre-inflammation responses (Scheffé's test, $P < 0.001$ and $P < 0.001$, respectively). A markedly different result was found in VR1^{-/-} mice. In these animals, withdrawal latencies of inflamed paws were indistinguishable from those measured before carrageenan injection (Scheffé's test, $P = 0.955$, Fig. 4c). Thus, knock out of VR1 eliminated the generation of a thermal hyperalgesic response. The contralateral paw showed no significant changes in response latency for the VR1^{-/-} and VR1^{+/-} mice, but there was an increase compared with baseline values in contralateral latencies in VR1^{+/+} mice. This may reflect a chance finding or the onset of an endogenous inhibitory drive resulting in hypoalgesia in the uninflamed contralateral paw (Fig. 4d).

These data highlight a marked effect of VR1 deletion upon responsiveness to noxious thermal stimuli where nociceptive pathways are sensitized (that is, during inflammation), and contrast with the situation in the naive mouse where thermal nociception is relatively unchanged. Pharmacological experiments using the VR1 antagonist capsazepine have also demonstrated an antihyperalgesic effect¹⁶. Selective VR1 antagonists may therefore prove effective for the treatment of thermal hyperalgesia.

Immunohistochemical and PCR analysis has identified VR1 expression in a wide range of brain regions and has led to suggestions that VR1 might be involved in behaviours other than nociception^{3,17}. To screen for further behavioural phenotypes and examine the specificity of our observations, VR1^{-/-} mice were tested for overt behavioural phenotypes using the 'SHIRPA' tests¹⁸. This assessment included 38 behavioural observations, recording of spontaneous locomotor activity and a holeboard exploratory behaviour test; the data arising from the screen are available in the Supplementary Information. Also included in this screen was a test of mechanical nociception—a toe pinch test. No significant differences between VR1^{+/+} and VR1^{-/-} mice were observed in any of these tests. These negative data demonstrate the specificity of the phenotype resulting from VR1 disruption, and also exclude altered nociceptive responses occurring as a result of effects upon motor function.

Our data demonstrate the specificity of the VR1 knockout in terms of gross behavioural deficits and point to an essential or predominant role of VR1 in responses of sDRG neurons to capsaicin, extracellular acidification or heat. Observations of the activation of VR1 by these and other ligands, such as anandamide¹⁰, suggest that VR1 may also function in pain where these other mediators are the predominant agonists. Our experiments have focused upon thermal responses, however, and the results show conclusively that VR1 is essential for the development of sensitization to thermal stimuli during inflammation but not for the normal sensation of noxious heat. □

Methods

Targeting of VR1 gene and generation of mutant mice

A standard gene targeting approach was chosen to replace, in E14.1 ES cells, the DNA encoding amino acids 460–555 of mVR1 with the neomycin phosphotransferase gene (detailed methods are provided in Supplementary Information). A 2.3-kilobase (kb) 3'

and 3.75-kb 5' homology arm were isolated from a mouse 129SVJ BAC library, cloned either side of PGKneo, and flanked by Diphtheria toxin-A gene as a negative selection marker¹⁹. Homologous recombination in resistant ES cells was confirmed by Southern blot and a multiplex PCR genotyping procedure^{20,21}. Three targeted clones were injected into C57Bl6/J-derived blastocysts, and the resulting chimaeras produced germline offspring. Males heterozygous for the mutated allele were mated to C57Bl6/J females and mutant progeny were intercrossed to generate an N1F1 study population. All experiments were conducted according to the requirements of the United Kingdom Animals (Scientific Procedures) Act (1986) and conformed to the ethical standards of SmithKline Beecham Pharmaceuticals.

Electrophysiological recordings

Dissociated DRG cells were prepared from 8–10-day-old pups and cultured on glass coverslips² in DMEM with N2 supplements, 50 ng ml⁻¹ β-NGF, 0.05% bovine serum albumin, 100 U ml⁻¹ penicillin and streptomycin. Whole-cell patch-clamp recordings were made from sDRGs (≤22 μM diameter) with an Axopatch 200B amplifier controlled by the pClamp7 software suite (Axon Instruments). For analysis of ligand- and pH-gated current, all experiments were conducted at room temperature (23–25.5 °C) at a holding potential of -70 mV. The bath solution comprised (in mM) NaCl 130, KCl 5, CaCl₂ 2, MgCl₂ 1, glucose 30, HEPES-NaOH 25; pH 7.3. Corresponding pH 5.3 solutions were adjusted with HCl. To minimize the holding current, and thus the contribution of the 'non-specific' heat-gated currents, most of our recordings of heat-gated current were made in near symmetrical Cs⁺ concentrations, with extracellular Ba²⁺ substituted for Ca²⁺ and methanesulphonate as the predominant intracellular anion. However, essentially similar observations (data not shown) were also made in a population of recordings under the conditions above. Electrodes had a resistance of 2–7 MΩ when filled with (in mM): CsCl 140, MgCl₂ 4, EGTA 10, HEPES-CsOH 10; pH 7.3. Applications of agonists and room temperature to 54 °C temperature jumps were made using an automated fast-switching solution exchange system (Warner Instruments SF-77B; time for solution exchange ~30 ms), in a manner similar to that described elsewhere¹.

Behavioural studies

All tests were performed on male 6–9-week-old mice ($n = 10$). VR1^{-/-} and VR1^{+/+} littermates were used in the primary behavioural observation screen SHIRPA¹⁸, full experimental procedures for which are available at <http://www.mgu.har.mrc.ac.uk/mutabase/>. In addition, a 30-min spontaneous locomotor activity test and a 10-min holeboard test of exploratory activity were used²².

Hotplate test

Mice of each genotype ($n = 8–10$) were tested in a random and blind fashion for thermal nociception using a hotplate (Harvard Analgesia Meter, Harvard Instruments) maintained at 50 or 52.5 °C. Mice were observed for signs of nociception, that is, rapid fanning or licking of the paws. The response latency was recorded and results analysed using 2-way analysis in Statistica (Statsoft Inc.). Genotype and hotplate temperature were used as independent variables. Follow up analyses were carried out using Duncan's test.

Carrageenan-induced inflammation

The same cohort of mice ($n = 17–20$ per genotype) were tested for thermal hyperalgesia using described methods modified for mice¹⁴. Animals were habituated to the test apparatus. Baseline withdrawal latencies, to a focused radiant heat stimulus (Plantar Test Apparatus, Ugo Basile), were measured for each hindfoot. Carrageenan (0.025 mls, 2%) was injected sub-plantar into the left hindfoot, and paw-withdrawal latencies were measured for both hindfeet 4 h later. Paw volumes were measured using a plethysmometer (Linton Instruments). Results were expressed as mean latency (s) for paw withdrawal at baseline and after carrageenan injection. All data were log transformed to correct for heterogeneity of variances. Results were analysed in SAS (Statsoft Inc.) using a split plot analysis of variance. Genotype and measurement were used as independent variables. In both cases, follow up analysis was carried out using Scheffé's test, where appropriate²³. Errors shown represent standard errors of the mean.

Received 20 December 1999; accepted 14 April 2000.

- Caterina, M. J. *et al.* The capsaicin receptor: a heat-activated ion channel in the pain pathway. *Nature* **389**, 816–824 (1997).
- Tominaga, M. *et al.* The cloned capsaicin receptor integrates multiple pain-producing stimuli. *Neuron* **21**, 531–543 (1998).
- Szallasi, A. & Blumberg, P. M. Vanilloid (Capsaicin) receptors and mechanisms. *Pharmacol. Rev.* **51**, 159–211 (1999).
- Bevan, S. *et al.* Capsazepine: A competitive antagonist of the sensory neurone excitant capsaicin. *Br. J. Pharmacol.* **107**, 544–552 (1992).
- Wood, J. N. *et al.* Capsaicin-induced ion fluxes in dorsal root ganglion cells in culture. *J. Neurosci.* **8**, 3208–3220 (1988).
- Bevan, S. & Yeats, J. Protons activate a cation conductance in a sub-population of rat dorsal root ganglion neurones. *J. Physiol.* **433**, 145–161 (1991).
- Waldmann, R. *et al.* H⁺-gated cation channels. *Ann. NY Acad. Sci.* **868**, 67–76 (1999).
- Bevan, S. & Winter, J. Nerve growth factor (NGF) differentially regulates the chemosensitivity of adult rat cultured sensory neurones. *J. Neurosci.* **15**, 4918–4926 (1995).
- Ueno, S., Tsuda, M., Iwanaga, T. & Inoue, K. Cell type-specific ATP-activated responses in rat dorsal root ganglion neurones. *Br. J. Pharmacol.* **126**, 429–436 (1999).
- Zygmunt, P. M. *et al.* Vanilloid receptors on sensory nerves mediate the vasodilatory action of anandamide. *Nature* **400**, 452–457 (1999).

11. Cesare, P. & McNaughton, P. A novel heat-activated current in nociceptive neurons and its sensitization by bradykinin. *Proc. Natl Acad. Sci. USA* **93**, 15435–15439 (1996).
12. Nagy, I. & Rang, H. P. Similarities and differences between the responses of rat sensory neurons to noxious heat and capsaicin. *J. Neurosci.* **19**, 10647–10655 (1999).
13. Nagy, J. I. & Kooy, D. van der. Effects of neonatal capsaicin treatment on nociceptive thresholds in the rat. *J. Neurosci.* **3**, 1145–1150 (1983).
14. Caterina, M. J., Rosen, T. A., Tominaga, M., Brake, A. J. & Julius, D. A capsaicin-receptor homologue with a high threshold for noxious heat. *Nature* **398**, 436–441 (1999).
15. Hargreaves, K., Dubner, R., Brown, F., Flores, C. & Joris, J. A new and sensitive method for measuring thermal nociception in cutaneous hyperalgesia. *Pain* **32**, 77–88 (1988).
16. Kwak, J. Y., Jung, J. Y., Hwang, S. W., Lee, W. T. & Oh, U. A capsaicin-receptor antagonist, capsazepine, reduces inflammation-induced hyperalgesic responses in the rat: evidence for an endogenous capsaicin-like substance. *Neuroscience* **86**, 619–626 (1998).
17. Sasamura, T., Sasaki, M., Tohda, C. & Kuraishi, Y. Existence of capsaicin-sensitive glutamatergic terminals in rat hypothalamus. *Neuroreport* **9**, 2045–2048 (1998).
18. Rogers, D. C. *et al.* 'SHIRPA'—a comprehensive behavioural and functional analysis of mouse phenotype. *Mamm. Genome* **8**, 711–713 (1997).
19. Yagi, T. *et al.* A novel selection for homologous recombinants using diphtheria toxin A fragment gene. *Anal. Biochem.* **214**, 77–86 (1993).
20. Torres, R. M. & Kuhn, R. *Laboratory Protocols for Conditional Gene Targeting*. (Oxford Univ. Press, Oxford, 1997).
21. Hooper, M., Hardy, K., Handyside, A., Hunter, S. & Monk, M. HPRT-deficient (Lesch-Nyhan) mouse embryos derived from germline colonization by cultured cells. *Nature* **326**, 292–295 (1987).
22. Rogers, D. C. *et al.* Use of SHIRPA and discriminant analysis to characterise marked differences in the behavioural phenotype of six inbred mouse strains. *Behav. Brain Res.* **105**, 207–217 (1999).
23. Miliken, G. A. & Johnson, D. E. in *Analysis of Messy Data* 29–45 (Chapman & Hall, London, 1992).

Supplementary information is available on Nature's World-Wide Web site (<http://www.nature.com>) or as paper copy from the London editorial office of Nature.

Acknowledgements

The authors would like to acknowledge P. Hayes, J. Nation, S. Pickering and C. David for technical assistance, and S. Rastan, F. Walsh, M. Geppert and D. Simmons for valuable critique.

Correspondence or requests for materials should be addressed to J.B.D. (e-mail: John_B_Davis@sbphrd.com).

Glutamatergic synapses on oligodendrocyte precursor cells in the hippocampus

Dwight E. Bergles*, J. David B. Roberts†, Peter Somogyi† & Craig E. Jahr*

* Vollum Institute, L474, Oregon Health Sciences University, Portland, Oregon 97201, USA

† MRC Anatomical Neuropharmacology Unit, Department of Pharmacology, University of Oxford, Oxford OX1 3TH, UK

Fast excitatory neurotransmission in the central nervous system occurs at specialized synaptic junctions between neurons, where a high concentration of glutamate directly activates receptor channels. Low-affinity AMPA (α -amino-3-hydroxy-5-methyl isoxazole propionic acid) and kainate glutamate receptors are also expressed by some glial cells¹, including oligodendrocyte precursor cells (OPCs). However, the conditions that result in activation of glutamate receptors on these non-neuronal cells are not known. Here we report that stimulation of excitatory axons in the hippocampus elicits inward currents in OPCs that are mediated by AMPA receptors. The quantal nature of these responses and their rapid kinetics indicate that they are produced by the exocytosis of vesicles filled with glutamate directly opposite these receptors. Some of these AMPA receptors are permeable to calcium ions, providing a link between axonal activity and internal calcium levels in OPCs. Electron microscopic analysis revealed that vesicle-filled axon terminals make synaptic junctions with the

processes of OPCs in both the young and adult hippocampus. These results demonstrate the existence of a rapid signalling pathway from pyramidal neurons to OPCs in the mammalian hippocampus that is mediated by excitatory, glutamatergic synapses.

Oligodendrocytes in the mammalian central nervous system develop from a population of precursor cells during late gestational and early postnatal life², providing the insulating sheaths of myelin necessary for rapid conduction of action potentials along axons. These precursors or OPCs were identified anatomically as smooth protoplasmic astrocytes based on their unique stellate morphology³, and their properties have been studied both in culture (termed O-2A cells)^{4–6} and in acutely isolated tissue (termed glial precursors or complex cells)^{1,7}. Glutamate receptor activation in these cells inhibits their proliferation and maturation into oligodendrocytes⁸, and prolonged exposure to glutamate causes excitotoxic degeneration⁹. Despite the potential importance of this pathway in the development and regeneration of myelin, it is not known how these receptors are activated *in vivo*. Glutamate has been shown to reach other glial cells by diffusion from nearby synaptic clefts following vesicular release¹⁰, or by reverse transport along axons¹¹.

To determine how glutamate reaches AMPA receptors on OPCs, we made whole-cell patch-clamp recordings from OPCs in the hippocampus and measured their response to stimulation of afferent excitatory axons. OPCs located in the stratum radiatum region of area CA1 exhibited small Na⁺ currents, large A-type and delayed rectifier K⁺ currents, and did not fire action potentials (Fig. 1a) ($n = 28$). Electrical stimulation in stratum radiatum elicited inward currents in OPCs that had rapid kinetics (Fig. 1b). Cells with these properties had a stellate morphology, with thin, highly branched processes that extended from a small cell body (Fig. 1c). They were identified as OPCs by their immunoreactivity to NG2 (Fig. 1d, e, $n = 10/10$), a proteoglycan that is only expressed by OPCs in this region¹². These NG2-positive cells were immunonegative for glial fibrillary acidic protein ($n = 3/3$), while astrocytes recorded from under similar conditions were immunopositive ($n = 8/8$ groups of cells).

Paired stimuli produced currents in OPCs that were larger ($P2/P1 = 1.7 \pm 0.1$, $n = 16$) and exhibited fewer apparent failures following the second stimulus (Fig. 2a), similar to paired-pulse facilitation of excitatory postsynaptic currents (EPSCs) in CA1

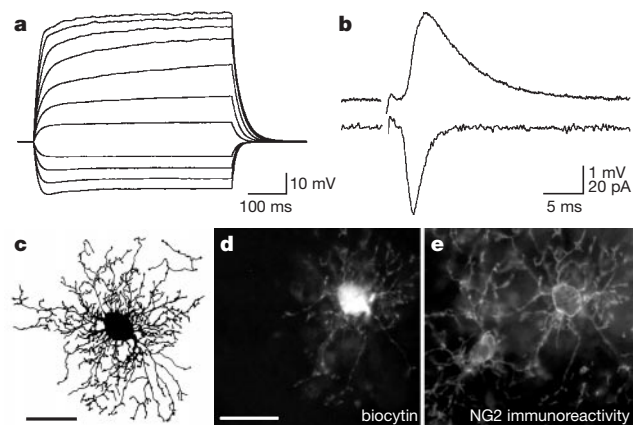


Figure 1 Synaptic responses from identified OPCs in hippocampal slices. **a**, Current-clamp recording of membrane responses to current injection (–80 to 140 pA; step size, 20 pA). **b**, Evoked responses to Schaffer collateral/commissural fibre stimulation, recorded in voltage-clamp (holding potential, –90 mV; lower trace) and current-clamp (membrane potential = –90 mV; upper trace). Traces are averages of 15 consecutive responses recorded from the same cell. Stimulus: 30 μ A, 100 μ s. **c**, Reconstruction of a biocytin-filled OPC. **d**, Micrograph of the same OPC as in **d**, visualized by AMCA-conjugated streptavidin. **e**, NG2-immunoreactivity of same region of the slice as shown in **d**. Scale bars for **c** and **d**, 20 μ m; **d** and **e** are at the same magnification.